Research Article

Journal of PeptideScience

Received: 1 February 2009 Revised: 6 March 2009 Accepted: 8 March 2009 Published online in Wiley Interscience: 27 April 2009

(www.interscience.com) DOI 10.1002/psc.1140

Synthesis of new modified truncated peptides and inhibition of glycogen phosphorylase

Stephanie S. Schweiker,[a] Wendy A. Loughlin,[a,b,*] Christopher L. Brown[a,b] and Gregory K. Pierens[c]

The first solution state structural analysis (NMR) of the C-terminal sequence of human G_L that binds to glycogen phosphorylase a (GPa), PEWPSYLGYEKLGPYY-NH_2 (1), showed it to be in a random coil conformation. This was supported by molecular dynamics simulation (modelled in solution) using NAMD 2.6. The conformational ambiguity of the peptide makes the structural arrangement of the peptide (and internal residues) strongly dependent on the environment. Thirteen tetra-peptide fragments of the C-terminal sequence, YEKLG-NH_2, and the corresponding tri- and di-peptide sequences were used in a fragment screen against GPa. Compound 2 (H-GPYY-NH_2) did not give an IC_{50} value, whereas PEWPSYLGYEKLGPYY-NH_2 (1) displayed an IC_{50} of 34 μM against GPa. Truncated peptides derived from 1, (EKL-NH_2, EKLG-NH_2, and AcEKNH_2) inhibited GPa (21%, 32%, 63%, respectively at 22 mM). These studies suggest key residues within the peptide chain have additional molecular interactions with GPa. The interaction of intra-sequence residues in combination with the terminal residues of PEWPSYLGYEKLGPYY with GPa may form the basis for the design of new inhibitors of GPa. Copyright © 2009 European Peptide Society and John Wiley & Sons, Ltd.

Supporting information may be found in the online version of this article

Keywords: glycogen phosphorylase; inhibition; peptide; NMR; circular dichroism

Introduction

GP [1,2] plays a crucial role in the conversion of glycogen to glucose-1-phosphate (and in turn glucose). Interest in GP as a therapeutic target has increased since it was validated in diabetic *ob/ob* mice [3]. Recently, emphasis towards discovery of new therapeutics for diabetes treatment has included allosteric inhibition as well as competitive inhibition of GP [4–6]. GP is a dimer of two identical subunits, existing in two forms: a relatively inactive b form (GPb) and a catalytically active a form (GPa). Each form has two conformations or states; an active (R) and inactive (T) state [1,7–9]. GPb exists predominantly in the T state and is converted to the highly active R state of GPa by phosphorylation at Ser-14 [7,8].

Homeostasis of glycogen is regulated by GPa and glycogen synthase activity. Glycogen synthase is activated by protein phosphatase 1 (PPP1) and is allosterically inhibited by binding of GPa to the glycogen-targeting subunit of PPP1 known as G_L [9–13]. The region of the G_L (PPP1R3B) subunit that binds to GPa has been identified as residues 269–284 (PEWPSYLGYEKLGPYY) [13] at the C-terminus end of G_L [11], and is absent from other glycogen-targeting subunits: G_M (PPP1R3A) [14], R5/PTG (PPP1R3C) [15,16], R6 (PPP1R3D) [17], PPP1R3E [18,19], PPP1R3F and PPP1R3G [20]. The sequence homologue of this region is conserved between mammalian species (rat, mouse, human), which suggests that allosteric regulation of GPa activity by G_L-PPP1 is important in mammals [11] and that G_L has the highest glycogenic potency [21]. In addition, G_L binding occurs in the presence of caffeine and glucose. As these substrates bind to unique sites that are homologous in muscle and liver phosphorylases, G_L is not binding at these sites. Recent work also has shown that a phosphorylase indole-2-carboxamide inhibitor, CP-316 819 blocks the interaction of GPa with the G_L C-terminus [22], and blocking of this interaction increases glycogen synthesis in primary rat hepatocytes [23]. These reports suggest that the G_L-PPP1 to GP interaction could be targeted in the development of a GPa inhibitor.

The molecular recognition of G_L-PPP1 by GP in the crystal state has been confirmed. In the solid state structure of GPa-G_L-Cterm 269–284G_L complex, only the terminal four amino acids (residues Gly281, Pro282, Tyr283, Tyr284) bound at the subunit interface, whereas the remainder of the peptide was disordered [24]. This was confirmed in solution where peptides (with the

* *Correspondence to: Wendy A. Loughlin, Eskitis Institute for Cell and Molecular Therapies, School of Biomolecular and Physical Sciences, Nathan Campus, Griffith University, Brisbane, QLD, 4111, Australia. E-mail: w.loughlin@griffith.edu.au*

a *Eskitis Institute for Cell and Molecular Therapies, Nathan Campus, Griffith University, Brisbane, QLD, 4111, Australia*

b *School of Biomolecular and Physical Sciences, Nathan Campus, Griffith University, Brisbane, QLD, 4111, Australia*

c *Centre for Magnetic Resonance, Gehrmann Laboratories, Research Rd, University of Queensland, Brisbane, QLD, 4072, Australia*

Abbreviations used: *BLAST, Basic Local Alignment Search Tool; DCM, dichloromethane; DIPEA, diisopropylethylamine; EDC.HCl, diethylcarbodiimide.hydrochloride; EGTA, ethylene glycol tetraacetic acid; GP, Glycogen Phosphorylase; gTOCSY, gradient Total Correlation Spectroscopy; HBTU; O-Benzotriazole-N,N,N′,N′-tetramethyluronium hexafluorophosphate; HOBt, 1-hydroxybenzotriazole; TFA, trifluoroacetic acid; TFE, 2,2,2-trifluoroethanol.*

Journal of PeptideScience

carboxyl C-terminal group intact) truncated to the C-terminal five to nine amino acids of G_L [22] and tetra- to hexa-peptides (GPYY, LGPYY, and KLGPYY) [24] all displayed binding affinities locating the interaction site to the last five residues. In addition, the two terminal tyrosines were shown to play a crucial role in binding [22,24]. However, we were curious that the truncated peptides with three or five residues removed (i.e. YLGYEKLGPYY and PSYLGYEKLGPYY) displayed comparable binding affinities to the 16 amino C-terminal peptide, and were more potent than the truncated peptides (see above) [22].

Action of an inhibitor on GP (*in vitro* or *in vivo*) generally occurs in solution. In the search for a new GPa inhibitor derived from PEWPSYLGYEKLGPYY, we sought to develop a better understanding of the solution state structure of the non-terminal section of PEWPSYLGYEKLGPYY-NH_2 (**1**). We also evaluated whether any other key structures contained within the non-terminal section of PEWPSYLGYEKLGPYY are required for inhibition of GPa, in the solution state. A fragment-screening [25,26] method using mapping of sequential sections of **1** was considered an effective approach. Throughout these studies a C-terminal amide group was used where possible, due to its stability, ease of synthesis, that it is removed from the internal residues of PEWPSYLGYEKLGPYY and that replacement of the terminal carboxylic acid group with a terminal amide group should remove a possible binding site and help to reveal whether any other interactions elsewhere in the peptide chain to GP are important.

Results and Discussion

Synthesis and Structural Aspects of PEWPSYLGYEKLGPYY-NH_2 1

PEWPSYLGYEKLGPYY-NH_2 (**1**) was prepared (3%) by solid-phase synthesis using Rink Amide NovaGel (load 0.50–0.70 mmol/g resin) and the Fmoc amino acids, where BOC (for Lys and Trp) and t-Bu (for Tyr, Glu, and Ser) were used as protecting groups. Purification by repeated reverse-phase HPLC (3 times) gave **1** in 99% purity but as a 19:3 epimeric mixture at the tryptophan residue, as determined by integration of the indole-NH signal in the ^{1}H NMR at 600 MHz and derived from the purity of the commercial supply of Fmoc-Trp(t-Bu)-OH. As the Trp residue was located near the N-terminus, the solution structure studies were carried out with the triply purified sample of **1**.

The ^{1}H NMR spectra of **1** was recorded and assigned using standard procedures from COSY, TOCSY, NOESY, HSQC, and HMBC spectra recorded in DMSO-d_6 at 295 K at 600 MHz. For the ^{1}H NMR spectra and chemical shift assignments of **1** see the Supporting Information. NMR spectra of **1** were also recorded in $CDCl_3$: DMSO-d_6 (3:2), However, NMR spectra of 1 in CD_3OD and D_2O were significantly less resolved than those obtained in DMSO-d_6. The assignment strategy was to identify residue side chains and assign the NH signals through analysis of the gTOCSY, followed by confirmation of assignments of **1** with gHSQC and gHMBC analysis. The resonances due to same amino-acid residues (i.e. Tyr6, Tyr9, Tyr15, and Tyr16; Pro4 and Pro14; Leu7 and Leu12, and Gly8 and Gly13) were co-incident and gave rise to severe spectral overlap. The synthetic linear sequence, where possible, was confirmed using gNOESY of all observed through space H–H correlations. Apart from correlations within a residue side chain, some NOE connections were identified that showed interactions between adjacent residues; for example, Trp3-ArH and Pro4-Hγ, Hδ; and Gly13-Hα and Pro14-Hδ. Interactions

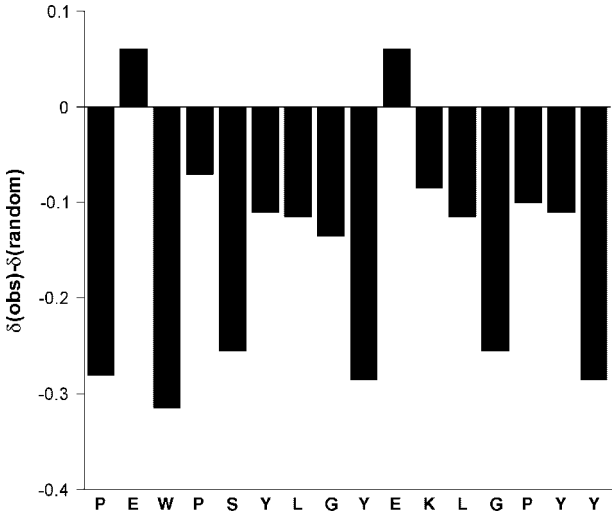

Figure 1. Plot of the differences between the observed Hα chemical shifts of the residues in **1** and the corresponding random coil values [28,29], δ (obs) – δ (random).

between non-adjacent residues were limited to a correlation between Trp3-ArH and Tyr6-*m*ArH, which was presumably a consequence of the intermediate proline residue Pro4, inducing a partial turn in the peptide chain. Ambiguities due to spectral overlap prevented a more complete analysis. Some conformational information was able to be obtained from the ^{1}H NMR spectrum of **1**. The measurable $^3J_{\alpha N}$ coupling constants, which can be related to the backbone dihedral angle phi, for Glu2, Trp3, Tyr6, Tyr9, Glu10, Tyr16 (terminal residue) were all determined to be ~7.4 Hz, consistent with a random coil conformation [27]. In addition, the Hα chemical shift deviations relative to random coil values [28] were determined (Figure 1), with the nearest-neighbour effect of proline taken into consideration [29]. The residues in the C and N termini are likely to be perturbed by ring current effects from Trp3, Tyr15, and Tyr16. The Hα chemical shift of residues Trp3 and Gly13 are likely shifted as result of preceding a proline residue [29]. The deviations of chemical shift from random coil values for 10 residues within the peptide chain are insignificant (~<0.1 ppm). The remaining six residues are not grouped in any patterned way that is suggestive of an alpha helix structure being present. Thus the Hα chemical shift analysis suggested overall that the peptide is unstructured, in the solution state.

Although most peptides as short as 16 residues can be expected to be unstructured in aqueous solutions, those that undergo induced-folding interactions often adopt structure in the presence of TFE [30]. The far UV CD spectra [31] of **1** in the range 190–250 nm was attempted in water (pH 8.15, 100%), in water/TFE solutions (95:5 to 10:90 with 5% increments), and in TFE (a helicogenic solvent [30]; 100%). Peptide **1** was totally soluble in the initial water solution, with the pH value lying within the physiological pH region (pH 5.0–8.5). In water, the far UV CD spectra values of **1** were of low intensity (despite dilution of **1**), and addition of the cosolvent TFE did not induce helicity in **1**. The CD spectra did not provide conclusive information on the solution state structure of **1**.

In the absence of an NMR structure of **1** in H_2O/D_2O *in silico* modelling in explicit solvent under periodic boundary conditions (to mimic physiological conditions) was carried out. The sequence function (PEWPSYLGYEKLGPYY) was confirmed, using a BLAST

Table 1. Inter-residue H-bond connectivity and percentage H-bond occupancy (during 5 ns) for the 16 residue sequence PEWPSYLGYEKLGPY

Entry	Residue 1 atom	Residue 2 atom	H-bond occupancy (%)	Interaction type
1	Glu2 C=**O**[a]	Tyr9 O–**H**[b]	5.6	Backbone (residue 1) and side chain (residue 2)
2	Ser5 N–**H**[c]	Gly8 C=**O**[a]	7.1	Backbone (residue 1) and backbone (residue 2)
3	Gly8 C=**O**[a]	Ser5 O–**H**[b]	5.8	Backbone (residue 1) and side chain (residue 2)
4	Tyr9 N–**H**[c]	Leu12 C=**O**[a]	13.3	Backbone (residue 1) and backbone (residue 2)
5	Lys11 C=**O**[a]	Tyr16 N–**H**[c]	8.9	Backbone (residue 1) and backbone (residue 2)
6	Gly13 N–**H**[c]	Tyr16 **O**–H[b]	5.7	Backbone (residue 1) and side chain (residue 2)
7	Gly13 N–**H**[c]	Tyr16 C=**O**[d]	9.5	Backbone (residue 1) and terminal (residue 2)

[a] O atom of the C=O group of the residue in the backbone.
[b] O atom of the OH group in residue side chain.
[c] H atom of the amide N–H group of the residue in the backbone.
[d] O atom of the C=O of the terminal group of the residue.

search (http://www.ncbi. nlm.nih.gov), as protein phosphatase 1, regulatory (inhibitor) subunit 3B (*Homo sapiens*) with the accession code of AAH43388. Submission of the last 25 amino acids from the C-terminal region (SPRCSYGLFPEWPSYLGYEKLGPY) against Swiss Model (http://swissmodel. expasy.org//SWISS-MODEL.html) returned no structural data. A secondary structure prediction from the PredictProtein site (http://cubic.bioc.columbia.edu/pp/) also indicated that this sequence would possess little secondary structural characteristics. To investigate the propensity of the sequence to adopt any form of secondary structural motif in solution a molecular dynamics study was carried out using the programs NAMD [32] and VMD [33]. Molecular dynamics simulation in explicit solvent under periodic boundary conditions at 380 K revealed that over a time course of 5 ns the sequence showed little susceptibility to adopt any secondary structural motif, further supporting the data from the CD and NMR studies. Of some interest, however, was that during the latter course of the simulation (from 2 ns onwards), several non-covalent interactions, in the form of semi-consistent hydrogen bond contacts, were observed between the backbone carbonyl oxygen atoms of Glu2, Gly8, Lys11, and the phenol OH group of Tyr9, side chain OH group of Ser5, and the backbone amide hydrogen atom of Tyr16, respectively (entries 1, 3 5; Table 1). Consistent hydrogen bond contacts also occurred between the backbone amide hydrogen atoms of Ser5, Tyr9, and the backbone carbonyl oxygen atoms of Gly8, Leu12 (entries 2, 4; Table 1), as well as between the backbone amide hydrogen atom of Gly13 and both (due to bond rotation) the terminal carbonyl oxygen atom of Tyr16 and phenol OH group of Tyr16, respectively (entries 6, 7; Table 1). The net result of these interactions was the formation of two well-defined loop regions within the sequence but during the course of the simulation no defined secondary structural characteristics, such as α-helix, were observed.

Synthesis of Short Peptides

Peptides **2**–**20** (Table 2) were synthesized using solid-phase peptide synthesis [34] using Rink Amide NovaGel (load 0.5–0.7 mmol/g resin), HBTU, DIPEA, and HOBt (3 equiv) and *N*-Fmoc amino acids that were side chain protected with *t*-butyl and BOC groups. The final crude peptides were obtained upon treatment of TFA to remove the protecting groups. Peptides were isolated by precipitation from cold ether (**2, 4**–**8, 13**–**17**) or hexane (**19**), room temperature ether (**9**–**12**) or ether with hexane (**3, 18, 20**). For compounds **21**–**24** (Table 2), the peptides were unable to be isolated after solid-phase synthesis due to their highly liphophilic structures and low molecular weight. Instead, standard peptide coupling (HOBt, EDC.HCl, DIPEA) [35] of Ac-Leu-OH **25** with Gly-OEt gave Ac-Leu-Gly-OEt [36] (**23**) (Scheme 1, Table 2), and subsequent hydrolysis of **23** with lithium hydroxide gave Ac-Leu-Gly-OH [36] (**24**) (Scheme 1, Table 2). Similarly, Ac-Lys(Z)-OH [37] **26** was coupled with Leu-OEt [38] to give Ac-Lys(Z)-Leu-OEt (**27**) (Scheme 2). *N*-benzoyl deprotection of **27** by hydrogenation gave Ac-Lys-Leu-OEt (**21**) (Scheme 2, Table 2). Hydrolysis of **21** with barium hydroxide and carbon dioxide [39] gave Ac-Lys-Leu-OH [40] (**22**) (Scheme 2, Table 2). Compounds **2**–**24** were purified by HPLC (**2**–**20**) or by recrystalization (**21**–**24**) and the purity (>98% pure) and characterization of the final peptides **2**–**24** was confirmed by ^{1}H and ^{13}C NMR spectroscopy, and HRMS (Table 2).

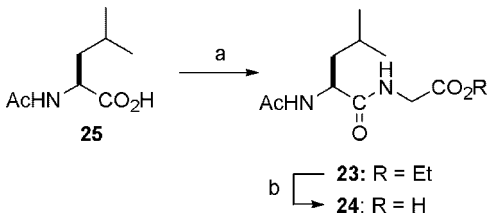

Scheme 1. Reagents and conditions: (a) HCl.NH_2-Gly-OEt, EDC.HCl, HOBt, DIPEA, room temperature 16 h, 60%; (b) LiOH, room temperature, 2 h, 90%.

Evaluation of Biological Activity

Compounds **1**–**24** were screened against GP as described [41] in the direction of glycogen synthesis by measuring the formation of inorganic phosphate from glucose-1-phosphate at 25 °C and against a caffeine standard, and were carefully monitored for signs of insolubility of the compound under assay conditions. The high concentration screening approach used here is aligned with 'fragment-screening' methods [25,26]. Data for inhibition of GPa by compounds **1**–**24** is summarized in Table 2. Synthetically derived compound **1** inhibited GPa at 34 μM, which compares favourably to the value obtained for the caffeine standard (283 ± 10 μM). This validated the assay and the purification techniques used for the peptides. Truncation of compound **1** into tetra-peptides gave compounds **2**–**14**. Screening of compounds **2**–**14** showed two peptides [compounds **5** (H-EKLG-NH_2) and **6** (H-YEKL-NH_2)] with low inhibition (10–32%) of GPa at 22 mM. Because of these moderate inhibition values, the Ki values were not determined. As both compounds **5** and **6** were consecutive

Journal of PeptideScience

Table 2. Peptide sequences, HRMS values, and percent inhibition of GPa

Cmpd. No.	Sequence	m/z[a] $(M+H)^+$ (ESI) observed	m/z[a] $(M+H)^+$ (ESI) calculated	% inhibition of GPa[b]
1	H-PEWPSYLGYEKLGPYY-NH_2[c]	1982.9295	1982.9299	$IC_{50} = 34 \pm 10$ μM
2	H-GPYY-NH_2	498.2376	498.2347	nc[d]
3	H-LGPY-NH_2	448.2539	448.2555	nc[d]
4	H-KLGP-NH_2	413.2863	413.2871	nc[d]
5	H-EKLG-NH_2	445.2785	445.2769	10 ± 2% at 22 mM
6	H-YEKL-NH_2	551.3219	551.3188	32 ± 2% at 22 mM
7	H-GYEK-NH_2	495.2567	495.2562	nc[d]
8	H-LGYE-NH_2	480.2465	480.2453	nc[d]
9	H-YLGY-NH_2	514.2649	514.2660	nc[d]
10	H-SYLG-NH_2	438.2352	438.2353	nc[d]
11	H-PSYL-NH_2	478.2664	478.2660	nc[d]
12	H-WPSY-NH_2[c]	551.2627	551.2613	nc[d]
13	H-EWPS-NH_2[c]	517.2410	517.2405	nc[d]
14	H-PEWP-NH_2[c]	527.2644	527.2613	nc[d]
15	H-YEKLG-NH_2	608.3400	608.3402	nc[d]
16	H-YEK-NH_2	438.2338	438.2347	16 ± 2% at 22 mM
17	H-EKL-NH_2	388.2558	388.2554	21 ± 2% at 22 mM
18	H-KLG-NH_2	316.2347	316.2343	nc[d]
19	Ac-YE-NH_2	374.1317	374.1322	nc[d]
20	Ac-EK-NH_2	317.1813	317.1819	63 ± 5% at 22 mM
21	Ac-KL-OEt	330.2392	330.2387	nc[d]
22	Ac-KL-OH	na[e]	na[e]	nc[d]
23	Ac-LG-OEt	na[e]	na[e]	nc[d]
24	Ac-LG-OH	na[e]	na[e]	nd[f]

[a] High-resolution mass spectroscopy using electrospray ionization method.
[b] % inhibition of GPa by peptide; values from 4 determinations±SD
[c] Commercially available Fmoc-Trp-OH contained an inseparable epimer (by HPLC).
[d] nc = not calculated; IC_{50} not reliably calculable with a maximum activity against GPa below 10% at maximal tested concentration of 22 m M.
[e] na = not applicable; literature compounds (**22**–**24**).
[f] nd = not determined, compound insoluble under assay conditions.

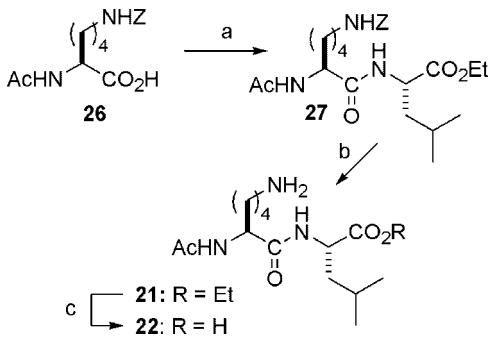

Scheme 2. Reagents and conditions: (a) H_2N-Leu-OEt, EDC.HCl, HOBt, DIPEA, room temperature, 16 h, 65%; (b) H_2, Pd-C, ethyl acetate, 48 h, 55%; (c) $Ba(OH)_2.H_2O$, 1 h then CO_2, 1 h, 90%.

within the sequence of compound **1**, further peptide variations of the YEKLG section were investigated. Screening of the di- and tri-peptides (compounds **16**–**24**) of the YEKLG section in addition to H-YEKLG-NH_2 (compound **15**), showed three peptides (compounds **16** (H-YEK-NH_2) and **17** (H-EKL-NH_2) with comparable (16–21%) or increased inhibition (63%; compound **20**; Ac-EK-NH_2 was *N*-acetylated to neutralize the N terminus) of GPa at 22 mM. In the absence of a binding terminal carboxyl group, the new peptides studied here show that low levels of inhibition of GPa (not binding) in solution, which appears to be generally associated with the residues Glu278, and Lys279. These two residues were common to all peptides that displayed a degree of inhibition (i.e. **1, 5, 6, 16, 17**, and **20**).

Conclusions

The solution structural studies revealed PEWPSYLGYEKLGPYY-NH_2 (**1**) (NMR, CD) and PEWPSYLGYEKLGPYY (modelling) to be in a random coil conformation. This has implications for the design of potential small molecule inhibitors of GP from sections of the peptide **1**. There appears to be no intrinsic propensity to adopt a defined secondary structure (such as α-helical region or β-turn) from which a scaffold could be designed. The conformational ambiguity of the peptide makes the structural arrangement of the peptide (and internal residues) strongly dependent on the environment. The results of the fragment screening of the di- to penta-peptides were interesting. Compound **2** (H-GPYY-NH_2) did not give an IC_{50} value, whereas PEWPSYLGYEKLGPYY-NH_2 (**1**) still displays an IC_{50} of 34 μM against GPa. This suggests that key residues within the peptide chain have additional (secondary?) molecular interactions leading to inhibition of GPa. This appears to be supported by the identification of residues in short peptides, which display a low level of inhibition of GPa. In the literature [22,24], the terminal residues of PEWPSYLGYEKLGPYY have been

identified as important in binding with GPa. In future work, the interaction of Glu278, and Lys279 in combination with the five terminal residues of PEWPSYLGYEKLGPYY may form the basis for the design of new inhibitors of GPa, however the site of interaction of inhibitors derived only from Glu278, and Lys279 would need to unambiguously established.

Materials and Methods

General

All solvents were of the highest purity. Rink Amide NovaGel (loading 0.50–0.70 mmol/g resin) and Fmoc protected amino acids were purchased from Merck Novabiochem. DCM was predried over calcium hydride and distilled under a nitrogen atmosphere before use. Water used for purification was MilliQ quality. All other reagents were purchased from Sigma Aldrich. Peptide bonds were formed using solution or solid phase chemistry and using EDC.HCl or HBTU, respectively, as the coupling reagents with the addition of HOBt in the presence of DIPEA. Solid-phase peptide synthesis was performed manually using solid-phase reaction vessel equipped with a coarse glass frit. The synthesis was monitored using the Kaiser Ninhydrin test. Other procedures were adopted from elsewhere [35]. Deprotection was carried out with piperidine (20% v/v in DMF), capping of unreacted amides with acetic anhydride, and side-chain deprotection and clevage from the resin with TFA in the presence of triisopropylsilane and distilled water (95 : 2.5 : 2.5). The product was precipitated using ether, or hexane and lyophilized to dryness. Final products were purified by reverse-phase HPLC using a Waters 486 tunable absorbance detector set at 215 nm and a Waters 600 controller with a Waters Spherisorb® 25 mm Module semi-preparative column (25 mm × 250 mm, 5 μm) and gradients of 0–100% acetonitrile in 0.1% aqueous TFA as a mobile phase (where solution A = MilliQWater with 0.1% TFA; solution B = acetonitrile with 0.1% TFA). Peptide purity was assessed by RP-HPLC using a Spherisorb® 25 mm Module semi-preparative column (25 mm × 250 mm, 7 μm) and the linear gradient of the same mobile phase for 60 min with UV detection at 215 nm, by ^{1}H NMR [Varian Unity 400 or a 600 MHz (Varian)] spectroscopy, with the samples dissolved in DMSO-d_6 or CD_3OD, and by electrospray ionization mass spectrometry (Fisons VG-Platform II spectrometer equipped with Mass Lynx Version II (IBM) software). HRMS were carried out at the University of Tasmania and Griffith University. The synthesis of Ac-Lys(Z)-OH [37] and Leu-OEt [38] was carried out according to literature procedures.

NMR Spectroscopy

^{1}H NMR spectra of peptides dissolved in DMSO-d_6 were recorded at 298 K at 400 MHz on a Varian Oxford Spectrometer. The ^{1}H NMR spectra of compound **1** dissolved in DMSO-d_6 was recorded at 298 K at 600 MHz on a Varian INOVA spectrometer equipped with a cold probe. The concentration of compound **1** was 0.96 mM in a sample volume of 570 μl. The one-dimensional spectra and the TOCSY and NOESY spectra of compound **1** were recorded with preirradiation of the water resonance. Typical 90° pulses were 6.0 μs (for 1D, TOCSY and NOESY spectra), with 80 and 200 ms mixing time for TOCSY and NOESY spectra, respectively. Typically, a sweep width of 13 ppm, with 2 K number of points being acquired; number increments = 256 and phase = 1,2 were used for the 2D experiments. The data was processed using a 90° shifted sine bell function in both directions.

Computational Methods

Starting Model

The target peptide (PEWPSYLGYEKLGPYY) was constructed using the protein builder module of Sirius (http://sirius.sdsc.edu) in a random starting conformation. This starting structure was saved as a PDB file and the structure then loaded into VMD 1.8.6 [33] whereupon a NAMD [32] input file was generated using the autopsf feature of VMD with included ions (to 0.5 mol^{-1} NaCl) and 5094 explicit (TIP3) water solvent molecules.

Modelling Procedures

The system was simulated under periodic boundary conditions using PME electrostatics as implemented in NAMD 2.6 [32]. The minimization step consisted of 1000 steps of minimization. Molecular dynamics was carried out at constant pressure (NTP) and the solute and solvent coupled to a constant temperature (T) 380 K. A residue-based cutoff distance of 15.5 Å was used for non-bonded interactions. The simulation ran for 5 ns on a Dell precision 490 workstation (8 core) running FC5.

Solid-Phase Peptide Synthesis

Rink Amide NovaGel (loading 0.50–0.70 mmol/g resin) was swelled in DCM (3ml, ×30 min). Nα-Fmoc amino acid (1.0 equiv) in DMF (3 ml), DIPEA (0.098 ml, 0.56 mmol, 4 equiv), HOBt (56.7 mg, 0.042 mmol, 3 equiv), and HBTU (154 mg, 0.41 mmol, 2.9 equiv) was added. The suspension was agitated for 30 min at room temperature, washed with DMF (3 ml × 5), DCM (3 ml × 5) and a Kaiser Ninhydrin test carried out. Acetic anhydride (50% v/v in DCM) was added, followed by washing with DCM (3 ml × 5), DMF (3 ml × 5), DCM (3 ml × 5), and DMF (3 ml). Piperidine (20% v/v in DMF) was added (3 ml 2 × 10 min), followed by washing with DMF (3 ml × 5), DCM (3 ml × 5), DMF (3 ml) and a Kaiser Ninhydrin test carried out. The first residue was coupled twice (2 × 30 min). After complete elongation of the peptide, TFA in the presence of TIPS and distilled water (95 : 2.5 : 2.5) was added, the suspension stirred for 90 min at room temperature and filtered. The resin was washed with TFA in the presence of TIPS and distilled H_2O (95 : 2.5 : 2.5) for with 10 min stirring at room temperature. The cleavage solutions were combined and the peptide precipitated with diethyl ether (45 ml × 4) (compounds **1, 2, 4–8, 13–17**); diethyl ether (25 ml × 4) and hexane (20 ml × 4) (compounds **3, 18, 20**); hexane (45 ml × 4) (compound **19**) at 0 °C or diethyl ether (45 ml × 4) (compounds **9–12**) at room temperature. Precipitation was followed by centrifugation at 4000 rpm for 5 min (×4). The resulting peptides were lyophilized, purified by reverse-phase HPLC (where solution A = MilliQWater with 0.1% TFA; solution B = acetonitrile with 0.1% TFA) and lyophilized. Analysis by NMR spectroscopy indicated that the peptides were all 98 + % pure, apart from compounds containing Trp, which were 80% pure (after multiple HPLC purification; one peak by HPLC) due to an inseparable epimer present in the commercially available Fmoc-Trp-OH. After completion of the NMR studies, the peptides were dissolved three times in aqueous ammonia and the ammonia removed in vacuo to remove the TFA salts. This cycle was repeated three times, and then the sample was lyophilized to dryness before screening against GPa.

PEWPSYLGYEKLGPYY-NH_2 (1)

Reverse-phase HPLC (gradient: 70% solution A and 30% solution B to 32% solution B 68% solution A over 20 min, t_R = 2.6 min) gave **1** as a fluffy white solid (4 mg, 1.5%). ESI-MS (+ve) 982 $(MH)^{2+}$.

Journal of PeptideScience

GPYY-NH_2 (2)

Reverse-phase HPLC (gradient: 95% solution A and 5% solution B to 10% solution A and 90% solution B over 60 min; t_R = 20.50 min) gave **2** as a fluffy white solid (8 mg, 13%). ^{1}H NMR (600 MHz, DMSO-d_6) δ: 1.66–1.74 (m, 1H), 1.74–1.84 (m, 2H), 1.92–2.00 (m, 1H), 2.61–2.73 (m, 2H), 3.35 (s, 2H), 3.39–3.51 (m, 2H), 3.79 (s, 1H), 4.39–4.48 (m, 3H), 4.80–4.90 (m, 2H), 6.62 (m, 4H), 6.97 (m, 4H), 7.19 (s, 1H), 7.29 (s, 1H), 7.65 (d, 2H, J = 7.5 Hz), 7.97 (d, 1H, J = 7.95 Hz), 8.05 (s, 2H); MS (ESI) 520 $(MNa)^+$.

LGPY-NH_2 (3)

Reverse-phase HPLC (gradient: 95% solution A and 5% solution B to 10% solution A and 90% solution B over 60 min; t_R = 37.0 min) gave **3** as a fluffy white solid (15 mg, 26%). ^{1}H NMR (400 MHz, DMSO-d_6) δ: 0.86 (d, 3H, J = 5.8 Hz), 0.89 (3H, d, J = 5.8 Hz), 1.48–1.62 (m, 2H), 1.62–1.76 (m, 3H), 1.76–1.88 (m, 1H), 2.69–2.79 (m, 1H), 2.82–2.93 (m, 1H), 3.30–3.52 (m, 2H), 3.68 (brs, 1H), 3.8–3.9 (m, 1H), 3.97 (d, 1H, J = 5.8 Hz), 4.04 (d, 1H, J = 5.8 Hz), 4.25–4.35 (m, 2H), 6.6 (d, 2H, J = 7.8 Hz), 7.00 (d, 2H, J = 7.8 Hz), 7.16 (brs, 1H), 7.44 (brs, 1H), 7.78 (d, 1H, J = 16.8 Hz), 8.10 (m, 2H), 8.70 (t, 1H, J = 5.8 Hz), 9.18 (brs, 1H); MS (ESI) 448 $(MH)^+$.

KLGP-NH_2 (4)

Reverse-phase HPLC (gradient: 95% solution A and 5% solution B to 10% solution A and 90% solution B over 30 min, t_R = 13.0 min) gave **4** as a fluffy white solid (6 mg, 12%). ^{1}H NMR (600 MHz, DMSO-d_6) δ: 0.83 (d, 3H, J = 8.3 Hz), 0.89 (d, 3H, J = 8.3 Hz), 1.28–1.39 (m, 2H), 1.43–1.55 (m, 4H), 1.55–1.83 (m, 1H) 1.62–1.68 (m, 2H), 1.68–1.73 (m, 2H), 1.83–1.91 (m, 2H), 12H2H1.99–2.04 (m, 1H), 2.75 (s, 2H), 3.50–3.60 (m, 2H), 3.75–3.82 (m, 1H), 3.89 (d, 1H, J = 5.8 Hz), 3.92 (d, 1H, J = 5.8 Hz), 4.19 (dd, 1H, J = 2.4, 8.8 Hz), 4.38–4.49 (m, 1H), 7.31 (s, 2H), 7.70 (s, 1H), 8.08–8.16 (m, 3H), 8.50–8.56 (m, 1H); MS (ESI) 413 $(MH)^+$.

EKLG-NH_2 (5)

Reverse-phase HPLC (gradient: 95% solution A and 5% solution B to 75% solution A and 25% solution B over 25 min, t_R = 11.30 min) gave **5** as a fluffy white solid (49 mg, 87%). ^{1}H NMR (400 MHz, DMSO-d_6) δ: 0.79 (d, 3H, J = 6.5 Hz), 0.88 (3H, d, J = 6.5 Hz), 1.20–1.40 (m, 2H), 1.42–1.50 (m, 2H), 1.50–1.56 (m, 3H), 1.56–1.70 (m, 2H), 1.86–1.95 (m, 2H), 2.20–2.30 (m, 2H), 2.75 (s, 2H), 3.35 (s, 3H), 3.50–3.70 (m, 2H), 3.80–3.90 (m, 1H), 4.20–4.30 (m, 2H), 7.03 (s, 1H), 7.22 (s, 1H), 7.81 (brs, 2H), 8.07–8.10 (t, 1H, J = 6.5 Hz), 8.21–8.25 (d, 1H, J = 9.7 Hz), 8.60 (d, 1H, J = 9.7 Hz); MS (ESI) 445 $(MH)^+$.

YEKL-NH_2 (6)

Reverse-phase HPLC (gradient: 95% solution A and 5% solution B to 75% solution A and 25% solution B over 25 min, t_R = 17.0 min) gave **6** as a fluffy white solid (50 mg, 72%). ^{1}H NMR (400 MHz, DMSO-d_6) δ: 0.79 (d, 3H, J = 8.9 Hz), 0.86 (d, 3H, J = 8.9 Hz), 1.27–1.38 (m, 2H), 1.38–1.46 (m, 3H), 1.48–1.58 (m, 3H), 1.58–1.70 (m, 1H), 1.70–1.82 (m, 1H), 1.82–1.94 (m, 1H), 2.22–2.30 (m, 2H), 2.70–2.77 (m, 2H), 2.70–2.80 (m, 1H), 2.91–3.00 (m, 1H), 3.80–4.20 (m, 1H), 4.18–4.28 (m, 2H), 4.34–4.41 (dd, 1H, J = 6.0, 6.0 Hz), 6.65–6.70 (d, 2H, J = 9.5 Hz), 6.95 (brs, 1H), 7.00–7.04 (d, 2H, J = 9.5 Hz), 7.35 (brs, 1H), 7.74 (brs, 3H), 7.89–7.91 (d, 1H, J = 9.5 Hz), 8.00 (brs, 3H), 8.15–8.20 (d, 1H, J = 9.5 Hz), 8.65 (d, 1H, J = 9.5 Hz); MS (ESI) 551 $(MNa)^+$.

GYEK-NH_2 (7)

Reverse-phase HPLC (gradient: 95% solution A and 5% solution B to 20% solution A and 80% solution B over 25 min, t_R = 12.0 min) gave **7** as a fluffy white solid (50 mg, 72%). ^{1}H NMR (600 MHz, DMSO-d_6) δ: 1.22–1.38 (m, 2H), 1.49–1.57 (m, 3H), 1.62–1.71 (m, 1H), 1.71–1.80 (m, 1H), 1.84–1.94 (m, 1H), 2.21–2.27 (m, 2H), 2.61–2.63 (m, 1H), 2.69–2.77 (m, 2H), 2.93–3.00 (dd, 1H, J = 4.0, 16.0 Hz), 3.35 (s, 2H), 3.42–3.44 (m, 1H), 3.52–3.59 (d, 1H), 4.21–4.24 (m, 1H), 4.24–4.28 (m, 1H), 4.49–4.53 (m, 1H), 6.63 (s, 2H), 6.99 (s, 2H), 7.33 (s, 1H), 7.72 (d, 1H, J = 6.7 Hz), 7.73 (s, 2H), 7.92 (s, 2H), 8.37 (d, 1H), 8.60 (d, 1H), 9.22 (s, 1H); MS (ESI) 495 (MH)+, 517 $(MNa)^+$.

LGYE-NH_2 (8)

Reverse-phase HPLC (gradient: 95% solution A and 5% solution B to 10% solution A and 90% solution B over 30 min, t_R = 12.30 min) gave **8** as a fluffy white solid (21 mg, 38%). ^{1}H NMR (600 MHz, DMSO-d_6) δ: 0.84 (d, 3H, J = 7.4 Hz), 0.87 (3H, d, J = 7.4 Hz), 1.42–1.58 (m, 2H), 1.60–1.68 (m, 1H), 1.71–1.80 (m, 1H), 1.84–1.94 (m, 1H), 2.19–2.22 (m, 2H), 2.61–2.68 (m, 1H), 2.84–2.94 (m, 1H), 3.64–3.71 (m, 3H), 3.63 (brs, 1H) 4.13–4.20 (m, 1H), 4.41–4.51 (m, 1H), 6.62 (d, 2H, J = 4.5 Hz), 7.01 (d, 2H, J = 4.5 Hz), 7.18 (s, 1H), 8.06 (d, 2H, J = 6.7 Hz), 8.09 (s, 1H), 8.13 (d, 1H, J = 8.8 Hz), 8.65 (t, 1H, J = 6.7 Hz), 9.22 (s, 2H); MS (ESI) 437 $(MH)^+$.

YLGY-NH_2 (9)

Reverse-phase HPLC (gradient: 95% solution A and 5% solution B to 10% solution A and 90% solution B over 30 min, t_R = 18.0 min) gave **9** as a fluffy white solid (4 mg, 7%). ^{1}H NMR (600 MHz, DMSO-d_6) δ: 0.82 (d, 3H, J = 6.9 Hz), 0.88 (3H, d, J = 6.9 Hz), 1.43–1.50 (m, 2H), 1.56–1.64 (m, 2H), 2.62–2.70 (m, 1H), 2.72–2.80 (m, 1H), 2.82–2.90 (m, 2H), 2.96–3.02 (m, 1H), 3.59–3.67 (m, 1H), 3.69–3.76 (m, 1H), 3.93 (s, 1H), 4.3–4.39 (m, 2H), 6.62 (d, 2H, J = 8.1 Hz), 6.69 (d, 4H, J = 8.1 Hz), 7.02 (d, 2H, J = 8.1 Hz), 7.88 (d, 2H, J = 8.1 Hz), 7.98 (s, 2H), 8.18 (t, 1H, J = 4 Hz), 8.59 (d, 2H, J = 8.1 Hz); MS (ESI) 513 $(MH)^+$.

SYLG-NH_2 (10)

Reverse-phase HPLC (gradient: 95% solution A and 5% solution B to 10% solution A and 90% solution B over 30 min, t_R = 14.30 min) gave **10** as a fluffy white solid (33 mg, 60%). ^{1}H NMR (400 MHz, DMSO-d_6) δ: 0.81 (d, 3H, J = 7.6 Hz), 0.86 (d, 3H, J = 7.6 Hz), 1.40–1.50 (m, 1H), 1.50–1.60 (m, 1H), 2.45 (s, 1H), 2.61–2.63 (d, 1H, J = 8.0 Hz), 2.93–3.00 (d, 1H, J = 8.0 Hz), 3.56–3.69 (m, 3H), 3.73–3.81 (m, 2H), 4.20–4.30 (m, 1H), 4.35–4.40 (m, 1H), 4.49–4.53 (m, 1H), 6.63 (s, 2H), 6.99 (s, 2H), 7.15 (s, 1H), 7.91 (s, 1H), 8.16 (s, 3H), 8.19 (d, 1H, J = 8.0 Hz), 8.60 (d, 1H, J = 8.0 Hz), 9.20 (brs, 1H); MS (ESI) 437 (MH)+, 460 $(MNa)^+$.

PSYL-NH_2 (11)

Reverse-phase HPLC (gradient: 95% solution A and 5% solution B to 10% solution A and 90% solution B over 30 min, t_R = 16.0 min) gave **11** as a fluffy white solid (15 mg, 25%). ^{1}H NMR (400 MHz, DMSO-d_6) δ: 0.83 (d, 3H, J = 7.4 Hz), 0.88 (d, 3H, J = 7.4 Hz), 1.40–1.45 (m, 2H), 1.50–1.51 (m, 1H), 1.70–1.90 (m, 2H), 2.20–2.30 (m, 2H), 2.70 (dd, 1H, J = 3.7, 18.5 Hz), 2.95 (dd, 1H, J = 7.4, 22.2 Hz), 3.10–3.30 (brs, 2H), 3.50–3.60 (m, 4H), 4.12–4.22 (m, 2H), 4.35–4.41 (m, 2H), 5.20 (brs, 1H), 6.60 (d, 2H, J = 14.0 Hz), 7.01 (d,

2H, $J = 14.0$ Hz), 7.90 (d, 1H, $J = 9.4$ Hz), 8.10 (d, 1H, $J = 9.4$ Hz), 8.50 (brs, 1H), 8.62 (d, 1H), 9.20 (brs, 1H); MS (ESI) 478 (MH)+, 500 $(MNa)^+$.

WPSY-NH_2 (12)

Reverse-phase HPLC (gradient: 95% solution A and 5% solution B to 10% solution A and 90% solution B over 30 min, $t_R = 16.30$ min) gave **12** as a fluffy white solid (15 mg, 22%). ^{1}H NMR (400 MHz, DMSO-d_6) δ: 1.69–1.88 (m, 3H), 1.98–2.08 (m, 1H), 2.68–2.78 (m, 1H), 2.89–2.99 (m, 1H), 3.02–3.22 (m, 2H), 3.48–3.52 (m, 1H), 3.52–3.61 (m, 2H) 3.61–3.66 (m, 1H), 4.21–4.31 (m, 2H), 4.31–4.38 (m, 1H), 4.42–4.49 (m, 1H), 5.20 (brs, 1H), 6.59–6.65 (m, 2H), 6.96–7.06 (m, 2H), 7.06–7.12 (m, 1H), 7.15 (s, 1H), 7.28 (s, 1H), 7.32–7.40 (m, 1H), 7.60 (d, 1H, $J = 7.3$ Hz), 8.16 (s, 1H), 8.5 (brs, 1H), 9.15 (s, 2H), 9.20 (brs, 1H), 11.03 (s, 1H); MS (ESI) 513 $(MH)^+$.

EWPS-NH_2 (13)

Reverse-phase HPLC (gradient: 95% solution A and 5% solution B to 10% solution A and 90% solution B over 30 min, $t_R = 16.30$ min) gave **13** as a fluffy white solid (30 mg, 46%). ^{1}H NMR (400 MHz DMSO-d_6) δ: 1.80–2.00 (m, 5H), 2.00–2.09 (m, 1H), 2.30–2.40 (m, 2H), 2.90–3.00 (dd, 1H, $J = 5.8$, 17.4 Hz), 3.15–3.23 (dd, 1H, $J = 8.7$, 20.0 Hz), 3.40–3.45 (m, 1H), 3.55–3.65 (m, 3H), 3.78 (m, 1H), 4.15–4.20 (m, 1H), 4.40 (dd, 1H, $J = 5.8$, 11.6 Hz), 4.70–4.80 (m, 1H), 4.87 (brs, 1H), 6.90–7.11 (m, 2H), 7.29 (d, 1H, $J = 3.6$ Hz), 7.32 (d, 1H, $J = 7.3$ Hz), 7.60 (d, 1H, $J = 7.3$ Hz), 7.73 (d, 1H, $J = 7.3$ Hz), 8.15 (brs, 4H), 8.85 (d, 1H, $J = 7.3$ Hz), 10.90 (s, 1H), 12.40 (brs, 1H); ESI-MS (+ve) 517 $(MH)^+$.

PEWP-NH_2 (14)

Reverse-phase HPLC (gradient: 95% solution A and 5% solution B to 60% solution A and 40% solution B over 30 min, $t_R = 26.0$ min) gave **14** as a fluffy white solid (12 mg, 18%). ^{1}H NMR (600 MHz, DMSO-d_6) δ: 1.69–1.96 (m, 9H), 1.97–2.03 (m, 1H), 2.16–2.24 (m, 2H), 2.87–2.94 (m, 2H), 3.12–3.2 (m, 2H), 3.49–3.54 (m, 1H), 3.59–3.64 (m, 1H), 3.90 (brs, 1H), 4.12–4.19 (m, 1H), 4.22–4.27 (m, 1H), 4.30–4.37 (m, 1H), 4.65–4.71 (m, 1H), 6.88 (s, 1H), 6.94–6.98 (m, 1H), 7.02–7.06 (m, 1H), 7.16 (brs, 1H), 7.22 (s, 1H), 7.23 (s, 1H), 7.56 (d, 1H, $J = 6.6$ Hz), 8.26 (d, 1H, $J = 10.3$ Hz), 8.45 (brs, 1H), 8.54 (d, 1H, $J = 10.3$ Hz), 10.84 (brs, 1H); MS (ESI) 527 $(MH)^+$.

YEKLG-NH_2 (15)

Reverse-phase HPLC (gradient: 95% solution A and 5% solution B to 20% solution A and 80% solution B over 40 min, $t_R = 10.0$ min) gave **15** as a fluffy white solid (57 mg, 74%). YEKLG-NH_2. TFA ^{1}H NMR (400 MHz, DMSO-d_6) δ: 0.80 (d, 3H, $J = 6.6$ Hz), 0.85 (3H, d, $J = 6.6$ Hz), 1.25–1.35 (m, 2H), 1.40–1.50 (m, 2H), 1.50–1.60 (m, 2H), 1.60–1.70 (m, 1H), 1.70–1.78 (m, 3H), 1.80–1.90 (m, 1H), 2.20–2.30 (m, 2H), 2.70–2.80 (m, 3H), 2.90–3.00 (m, 1H), 3.50–3.60 (m, 2H), 3.99 (s, 1H), 4.20–4.30 (m, 2H), 4.30–4.40 (m, 1H), 6.60 (d, 2H, $J = 8.5$ Hz) 7.00 (d, 2H, $J = 8.5$ Hz), 7.22 (brs, 1H), 7.81 (2H, brs), 8.00–8.11 (m, 2H), 8.19 (d, 1H, $J = 6.4$ Hz), 8.66 (d, 1H, $J = 8.5$ Hz); MS (ESI) 609 $(MH)^+$.

YEK-NH_2 (16)

Reverse-phase HPLC (gradient: 95% solution A and 5% solution B to 65% solution A and 35% solution B over 5 min, then 20% solution A and 80% solution B over 25 min, $t_R = 13.0$ min) gave **16** as a white foam (48 mg, 87%). YEK-NH_2. TFA ^{1}H NMR (400 MHz, DMSO-d_6) δ: 1.20–1.40 (m, 2H), 1.40–1.60 (m, 2H), 1.60–1.65 (m, 2H), 1.65–1.80 (m, 1H), 1.80–2.00 (m, 1H), 2.20–2.40 (m, 2H), 2.70–2.85 (m, 3H), 2.90–3.00 (m, 1H), 3.90–4.10 (brs, 1H), 4.15–4.20 (m, 1H), 4.25–4.40 (m, 1H), 6.70 (d, 1H, $J = 10.9$ Hz), 7.05 (d, 1H, $J = 10.9$ Hz), 7.49 (s, 1H), 7.80 (s, 1H), 8.15 (d, 1H, $J = 8.4$ Hz), 8.65 (d, 2H, $J = 8.4$ Hz); MS (ESI) 438 $(MH)^+$.

EKL-NH_2 (17)

Reverse-phase HPLC (gradient: 95% solution A and 5% solution B to 40% solution A and 60% solution B over 20 min, $t_R = 9.0$ min) gave **17** as a white foam (44 mg, 90%). EKL-NH2. TFA ^{1}H NMR (400 MHz, DMSO-d_6) δ: 0.90 (3H, d, $J = 6.6$ Hz), 0.95 (3H, d, $J = 6.6$ Hz), 1.10–1.20 (m, 2H), 1.20–1.30 (m, 2H), 1.30–1.40 (m, 3H), 1.40–1.55 (m, 2H), 1.80–2.00 (m, 2H), 2.15–2.20 (m, 2H), 2.7–2.8 (m, 2H), 3.80–3.90 (m, 1H), 4.21–4.25 (m, 1H), 4.25–4.32 (m, 1H), 6.95 (s, 1H), 7.19 (s, 1H), 7.81 (s, 2H), 8.15 (d, 1H, $J = 7.4$ Hz), 8.20 (s, 1H), 8.60 (d, 1H, $J = 7.4$ Hz); MS (ESI) 389 $(MH)^+$.

KLG-NH_2 (18)

Reverse-phase HPLC (gradient: 95% solution A and 5% solution B to 20% solution A and 80% solution B over 40 min, $t_R = 9.0$ min) gave **18** as a white foam (11 mg, 28%). KLG-NH2. TFA ^{1}H NMR (400 MHz, DMSO-d_6) δ: 0.90 (d, 3H, $J = 7.0$ Hz), 0.95 (d, 3H, $J = 7.0$ Hz), 1.20–1.40 (m, 2H), 1.40–1.60 (m, 4H), 1.60–1.80 (m, 3H), 2.70 (brs, 2H), 3.70 (t, 1H, $J = 6.4$ Hz), 3.80 (brs, 1H), 4.30–4.40 (m, 1H), 7.00 (brs, 1H), 7.22 (brs, 1H), 7.8 (brs, 2H), 8.20 (brs, 2H), 8.25–8.30 (m, 1H), 8.57 (d, 1H, $J = 11.0$ Hz); MS (ESI) 316 $(MH)^+$.

Ac-YE-NH_2 (19)

Reverse-phase HPLC (gradient: 95% solution A and 5% solution B to 20% solution A and 80% solution B over 40 min, $t_R = 11.0$ min) gave **19** as a white foam (18 mg, 41%). ^{1}H NMR (300 MHz, DMSO-d_6) δ: 1.60–1.80 (m, 4H), 1.82–2.00 (m, 1H), 2.15–2.25 (m, 2H), 2.45–2.65 (m, 1H), 2.80–2.95 (m, 1H), 4.10–4.20 (m, 1H), 4.30–4.40 (m, 1H), 6.62 (d, 1H, $J = 7.9$ Hz), 7.02 (d, 1H, $J = 7.9$ Hz), 7.16 (s, 1H), 7.93 (d, 1H, $J = 7.9$ Hz), 8.02 (d, 1H, $J = 7.9$ Hz); MS (ESI) 351 $(MH)^+$.

Ac-EK-NH_2 (20)

Reverse-phase HPLC (gradient: 95% solution A and 5% solution B to 20% solution A and 80% solution B over 40 min, $t_R = 5.3$ min) gave **20** as a white foam (20 mg, 50%). ^{1}H NMR (300 MHz, DMSO-d_6) δ: 1.20–1.33 (m, 2H), 1.45–1.55 (m, 3H), 1.60–1.70 (m, 2H), 1.70–1.90 (m, 4H), 2.20–2.30 (t, 2H, $J = 7.5$ Hz), 2.70–2.80 (m, 2H), 4.05–4.08 (m, 1H), 4.08–4.12 (m, 1H), 7.02 (s, 1H), 7.28 (s, 1H), 7.73 (brs, 2H), 7.88 (d, 1H, $J = 9$ Hz), 7.06 (d, 1H, $J = 7.3$ Hz); MS (ESI) 317 $(MH)^+$.

Synthesis of Short Peptides

Ac-K(Z)L-OEt (27)

HOBt (45 mg, 0.34 mmol, 0.85 equiv), and EDC.HCl (76 mg, 0.4 mmol, 1 equiv) was added to a solution of Ac-Lys(Z)-OH (129 mg, 0.4 mmol, 1 equiv) in DMF (6 ml) under a nitrogen atmosphere and the solution stirred for 2 h at room temperature. NH_2-Leu-OEt (95 mg, 0.6 mmol, 1.5 equiv) and DIPEA (18 ml, 2.5 equiv) were added and the solution stirred for 18 h at room

Journal of PeptideScience

temperature. HCl (2 M, 30 ml) was added and the aqueous phase extracted with ethyl acetate (3 × 30 ml). The combined organic phases were washed with brine (3 × 30 ml), dried ($MgSO_4$, anhydrous) and the solvent removed in vacuo to give a yellow oil. The oil was purified by silica gel chromatography (ethyl acetate/methanol/triethyl amine 89 : 10 : 1) to give **27** (139 mg, 65%) as a yellow oil in 90% purity, which was used directly in the next step. ^{1}H NMR (300 MHz, $CDCl_3$) δ: 0.81 (3H, d, J = 7.5 Hz), 0.85 (3H, d, J = 7.5 Hz), 1.07–1.20 (m, 3H), 1.22–1.35 (m, 2H), 1.35–1.45 (m, 2H), 1.45–1.65 (m, 4H), 1.65–1.80 (m, 1H), 1.88 (s, 3H), 2.98–3.15 (m, 2H), 3.96–4.11 (m, 2H), 4.35–4.45 (m, 1H), 4.45–4.55 (m, 1H), 5.00 (s, 2H), 5.20 (t, 0.5H, J = 4.0 Hz), 5.41 (t, 0.5H, J = 4.0 Hz), 6.80 (t, 1H, J = 6.5 Hz), 7.30 (s, 5H), 7.35 (d, 1H, J = 7.0 Hz). MS (ESI) 486 $(MNa)^+$.

Ac-KL-OEt (21)

Ac-K(Z)L-OEt (439 mg, 0.946 mmol) was dissolved in ethyl acetate (30 ml) and added to Pd-C (330 mg, 10%, 75% w/w) under nitrogen atmosphere. Ethyl acetate (70 ml) was added the mixture placed under a hydrogen atmosphere for 48 h. The reaction was quenched with N_2 and celite added. The mixture was filtered and solvent removed in vacuo to give a yellow oil. The oil was dissolved in methanol and precipitated with hexane to give **21** (171 mg, 55%) as a yellow oil. ^{1}H NMR (300 MHz, $CDCl_3$) δ: 0.78–0.91 (6H, m), 1.22 (t, 3H, J = 6.7 Hz), 1.28–1.42 (m, 2H), 1.42–1.78 (m, 5H), 1.78–1.88 (m, 2H), 1.96 (d, 3H, J = 4.5 Hz), 2.62–2.72 (m, 2H), 4.04–4.18 (m, 2H), 4.39–4.51 (m, 2H), 6.98 (t, 1H, J = 12.5 Hz), 7.48 (t, 1H, J = 10 Hz). MS (ESI) 330 $(MH)^+$.

Ac-KL-OH (22)

Ac-KL-OEt (50 mg, 1 equiv) was dissolved in THF (0.5 ml), added to $Ba(OH)_2.H_2O$ (144 mg, 5 equiv) in water (3 ml) and stirred at room temperature for 1 h. Carbon dioxide was bubbled through the reaction mixture for 1 h, the precipitate was removed by filtration and washed with water. The water layer was lyophilized to dryness. The residue was dissolved in methanol (10 ml) filtered and concentrated in vacuo. Recrystallization (methanol/hexane) gave pure **22** [40] (45 mg, 90%) as a white gum. ^{1}H NMR (300 MHz, CD_3OD) δ: 0.80–0.88 (m, 6H), 1.30–1.44 (m, 2H), 1.44–1.62 (m, 5H), 1.62–1.77 (m, 2H), 1.89 (d, 3H, J = 8.8 Hz), 2.77–2.85 (m, 2H), 4.17–4.29 (m, 2H). MS (ESI) 300 $(M)^-$.

Ac-LG-OEt (23)

HOBt (133 mg, 0.98 mmol, 0.85 equiv) and EDC.HCl (222 mg, 0.116 mmol, 1 equiv) were added to a solution of Ac-Leu-OH (200 mg, 0.116 mmol, 1 equiv) in DMF (6 ml) under a nitrogen atmosphere and the solution stirred for 2 h at room temperature. $HCl.NH_2$-Gly-OEt (179 mg, 1.7 mmol, 1.5 equiv) was added to DIPEA (0.3 ml, 1.7 mmol, 1.5 equiv) in DMF (0.5 ml) and stirred under a nitrogen atmosphere at room temperature for 30 min. The second solution was then added to the first solution and DIPEA (0.4 ml, 2.3 mmol, 2.5 equiv) was added. The reaction mixture was stirred under nitrogen for 18 h at room temperature, HCl (2 M, 30 ml) was added. The aqueous phase was extracted with ethyl acetate (3 × 30 ml). The combined organic phases were washed with brine (3 × 30 ml), dried ($MgSO_4$, anhydrous) and the solvent was removed in vacuo to give a white solid. The solid was purified by silica gel chromatography (gradient starting with DCM/ethyl acetate/triethyl amine 80 : 20:0.5 to DCM/ethyl acetate/isopropyl alcohol/triethyl amine 48 : 48 : 5 : 0.5). Recrystallization (methanol/diethyl ether) gave pure **23** [36] (25 mg, 60%) as a white solid MP 99–100 °C. (Lit [36]. MP 100–101 °C) ^{1}H NMR (300 MHz, $CDCl_3$) δ: 0.91 (d, 3H, J = 7.8 Hz), 0.95 (d, 3H, J = 7.8 Hz), 1.35 (t, 3H, J = 4.6 Hz), 1.50 (t, 1H, J = 5.7 Hz), 1.60–1.70 (m, 2H), 2.00 (s, 3H), 3.98 (q, 2H, J = 4.8 Hz), 4.49–4.55 (m, 1H), 6.18 (d, 1H, J = 5.3 Hz), 6.8 (s, 1H). MS (ESI) 281 $(MNa)^+$.

Ac-LG-OH (24)

Ac-LG-OEt (340 mg) and LiOH (8 ml) were added to THF (2 ml) and stirred under nitrogen for 2 h at room temperature. LiOH (30 ml) was added and the aqueous phase extracted with ethyl acetate (3 × 30 ml) was discarded. The aqueous phases was acidified to pH 1 and extracted with ethyl acetate (3 × 30 ml). The combined ethyl acetate layers were washed with brine (3 × 30 ml), dried ($MgSO_4$, anhydrous) and the solvent was removed in vacuo to give a white solid. The solid was recrystallized (methanol/diethyl ether) to give a pure **24** [36] (273 mg, 90%) as a white solid MP 192–196 °C. (Lit [36]. MP 193–194 °C) ^{1}H NMR (300 MHz, CD_3OD) δ: 0.91 (d, 3H, J = 7.7 Hz), 0.95 (d, 3H, J = 7.7 Hz), 1.50–1.80 (m, 3H), 2.00 (s, 3H), 3.98 (dd, 2H, J = 10.7, 21.0 Hz), 4.45 (q, 1H, J = 5 Hz). MS (ESI) 253 $(MNa)^+$; 229 $(M)^-$.

Biological Assay

Rabbit Muscle Glycogen Phosphorylase a (from Sigma, 0.475 µg/ml) activity was measured in the direction of glycogen synthesis by the release of phosphate from glucose-1-phosphate [42] using a 384 well plate at 22 °C in 45 µl of buffer containing 50 mM Hepes (pH 7.2), 100 mM KCl, 2.5 mM EGTA, 2.5 mM $MgCl_2$, 0.25 mM glucose-1-phosphate, and 1 mg/ml glycogen with a 30-min incubation time. Phosphate was measured at 620 nm, 5 min after the addition of 150 µl of 1 M HCl containing 10 mg/ml ammonium molybdate and 0.38 mg/ml malachite green [43]. Test compounds (obtained after HPLC and with TFA removed) were added to the assay in 5 µl of 14% DMSO. Compounds were tested against a caffeine standard in 11 point concentration–response curve in duplicate on two separate occasions. Data was analysed using GraphPad Prism v.4.03. A nonlinear regression (curve fit) analysis with a sigmoidal dose–response equation (variable slope) was applied to generate IC_{50} and Hill slope values. The reported IC_{50} had a Hill slope between 0.7 and 1.2 and a Z′ value of ~0.8. Compounds were screened with maximal concentrations of 0.22 mM (**1**–**14**) and 22 mM (**5, 6, 15**–**24**) and were monitored for signs of compound insolubility under assay conditions. Where an IC_{50} could not be determined, the percentage of inhibition observed at maximal concentration was reported. The results are presented as mean values from 4 determinations ±SD.

Supporting information

Supporting information may be found in the online version of this article.

Acknowledgements

The Financial support of (i) Diabetes Australia Research Trust (DART Grant 2007), (ii) Griffith University, (iii) Eskitis Institute for Cell and Molecular Therapies, Griffith University, (iv) the award of an APRS to S.S. Schweiker, (v) Deborah Wessling and Aaron

Lock from the Lead Discovery Biology section of Natural Product Discovery, Griffith University, for GPa assay, and (vi) Duong Luo for making freely available the H-bond occupancy analysis script (hbond_occupancy.tcl) used with VMD.

References

1 Bollen M, Keppens S, Stalmans W. Specific features of glycogen metabolism in the liver. *Biochem. J.* 1998; **336**: 19–31.
2 Johnson L. Glycogen phosphorylase: control by phosphorylation and allosteric effectors. *FASEB J.* 1992; **6**: 2274–2282.
3 Hoover D, Lefkowitz-Snow S, Burgess-Henry J, Martin W, Armento S, Stock I, McPherson R, Genereux P, Gibbs M, Treadway J. Indole-2-carboxamide inhibitors of human liver glycogen phosphorylase. *J. Med. Chem.* 1998; **41**: 2934–2938.
4 Henke B, Sparks S. Glycogen phosphorylase inhibitors. *Mini-Rev. Med. Chem.* 2006; **6**: 845–857.
5 Baker D, Greenhaff P, MacInnes A, Timmons J. The experimental type 2 diabetes therapy glycogen phosphorylase inhibition can impair aerobic muscle function during prolonged contraction. *Diabetes* 2006; **55**: 1855–1861.
6 Somsak L, Czifrak K, Toth M, Bokor E, Chrysina ED, Alexacou K-M, Hayes JM, Tiraidis C, Lazoura E, Leonidas DD, Zographos SE, Oikonomakos NG. New inhibitors of glycogen phosphorylase as potential antidiabetic agents. *Curr. Med. Chem.* 2008; **15**: 2933–2984.
7 Rath V, Ammirati M, Danley D, Ekstrom J, Gibbs E, Hynes T, Mathiowetz A, McPherson R, Olson T, Treadway J, Hoover D. Human liver glycogen phosphorylase inhibitors bind at a new allosteric site. *Chem. Biol.* 2000; **7**: 677–682.
8 Newgard C, Hwang P, Fletterick R. The family of glycogen phosphorylases: structure and function. *Crit. Rev. Biochem. Mol. Biol.* 1989; **24**: 69–99.
9 Alemany S, Cohen P. Phosphorylase a is an allosteric inhibitor of the glycogen and microsomal forms of rat hepatic protein phosphatase-1. *FEBS Lett.* 1986; **198**: 194–202.
10 Oikonomakos N. Glycogen phosphorylase as a molecular target for type 2 diabetes therapy. *Curr. Protein Pept. Sci.* 2002; **3**: 561–586.
11 Armstrong C, Doherty M, Cohen P. Identification of the separate domains in the hepatic glycogen-targeting subunit of protein phosphatase 1 that interact with phosphorylase a, glycogen and protein phosphatase 1. *Biochem. J.* 1998; **336**: 699–704.
12 Moorhead G, MacKintosh C, Morrice N, Cohen P. Purification of the hepatic glycogen-associated form of protein phosphatase-1 by microcystin-Sepharose affinity chromatography. *FEBS Lett.* 1995; **362**: 101–105.
13 Doherty M, Moorhead G, Morrice N, Cohen P, Cohen P. Amino acid sequence and expression of the hepatic glycogen-binding (GL)-subunit of protein phosphatase-1. *FEBS Lett.* 1995; **375**: 294–298.
14 Chen Y, Hansen L, Chen M, Bjorbaek C, Vestergaard H, Hansen T, Cohen P, Pedersen O. Sequence of the human glycogen-associated regulatory subunit of type 1 protein phosphatase and analysis of its coding region and mRNA level in muscle from patients with NIDDM. *Diabetes* 1994; **43**: 1234–1241.
15 Doherty M, Young P, Cohen P. Amino acid sequence of a novel protein phosphatase 1 binding protein (R5) which is related to the liver- and muscle-specific glycogen binding subunits of protein phosphatase 1. *FEBS Lett.* 1996; **399**: 339–343.
16 Printen J, Brady M, Saltiel A. PTG, a protein phosphatase 1-binding protein with a role in glycogen metabolism. *Science* 1997; **275**: 1475–1478.
17 Armstrong C, Browne G, Cohen P, Cohen P. PPP1R6, a novel member of the family of glycogen-targetting subunits of protein phosphatase 1. *FEBS Lett.* 1997; **418**: 210–214.
18 Munro S, Ceulemans H, Bollen M, Diplexcito J, Cohen P. A novel glycogen-targeting subunit of protein phosphatase 1 that is regulated by insulin and shows differential tissue distribution in humans and rodents. *FEBS J.* 2005; **272**: 1478–1489.
19 Munro S, Cuthbertson D, Cunningham J, Sales M, Cohen P. Human skeletal muscle expresses a glycogen-targeting subunit of PP1 that is identical to the insulin-sensitive glycogen-targeting subunit GL of liver. *Diabetes* 2002; **51**: 591–598.
20 Ceulemans H, Stalmans W, Bollen M. Regulator-driven functional diversification of protein phosphatase-1 in eukaryotic evolution. *BioEssays* 2002; **24**: 371–381.
21 Gasa R, Jensen P, Berman H, Brady M, DePaoli-Roach A, Newgard C. Distinctive regulatory and metabolic properties of glycogen-targeting subunits of protein phosphatase-1 (PTG, GL, GM/RGl) expressed in hepatocytes. *J. Biol. Chem.* 2000; **275**: 26396–26403.
22 Kelsall I, Munro S, Hallyburton I, Treadway J, Cohen P. The hepatic PP1 glycogen-targeting subunit interaction with phosphorylase a can be blocked by C-terminal tyrosine deletion or an indole drug. *FEBS Lett.* 2007; **581**: 4749–4753.
23 Zibrova D, Grempler R, Streicher R, Kauschke SG. Inhibition of the interaction between protein phosphatase 1 glycogen-targeting subunit and glycogen phosphorylase increases glycogen synthesis in rat primary hepatocytes. *Biochem. J.* 2008; **412**: 359–366.
24 Pautsch A, Stadler N, Wissdorf O, Langkopf E, Moreth W, Streicher R. Molecular recognition of the protein phosphatase 1 glycogen targeting subunit by glycogen phosphorylase. *J. Biol.Chem.* 2008; **283**: 8913–8918.
25 Leach A, Hann M, Burrows J, Griffen E. Fragment screening: an introduction. *Mol. Biosyst.* 2006; **2**: 429–446.
26 Fattori D. Molecular recognition: the fragment approach in lead generation. *Drug Discov. Today* 2004; **9**: 229–238.
27 Williamson M, Waltho J. Peptide structure from NMR. *Chem. Soc. Rev.* 1992; **21**: 227–236.
28 Merutka G, Dyson HJ, Wright PE. 'Random coil' 1H chemical shifts obtained as a function of temperature and trifluoroethanol concentration for the peptide series GGXGG. *J. Biomol. NMR* 1995; **5**: 14–24.
29 Wishart DS, Bigam CG, Hom A, Hodges RS, Sykes BD. ^{1}H, ^{13}C and ^{15}N random coil NMR chemical shifts of the common amino acids. I. Investigations of nearest-neighbour effects. *J. Biomol. NMR* 1995; **5**: 67–81.
30 Buck M. Trifluoroethanol and colleagues: cosolvents come of age. Recent studies with peptides and proteins. *Q. Rev. Biophys.* 1998; **31**: 297–355.
31 Woody R. Circular dichroism of peptides. *Peptides* 1985; **7**: 15–114.
32 Phillips JC, Braun R, Wang W, Gumbart J, Tajkhorshid E, Villa E, Chipot C, Skeel RD, Kale L, Klaus Schulten K. Scalable molecular dynamics with NAMD. *J. Comp. Chem.* 2005; **26**: 1781–1802.
33 Humphrey W, Dalke A, Schulten K. VMD – visual molecular dynamics. *J. Molec. Graphics* 1996; **14**: 33–38.
34 Chan W, White P. *Fmoc Solid Phase Peptide Synthesis: A Practical Approach*. Oxford University Press: New York, 2000.
35 Bodansky M. *Practice in Peptide Chemistry*. Springer-Verlag: Weinheim, 1984.
36 Smart N, Young G, Williams M. Amino acids and peptides. XV. Racemization during peptide synthesis. *J. Chem. Soc.* 1960; 3902–3912.
37 Irving C, Gutmann H. Preparation and properties of Nα-acyl lysine esters. *J. Org. Chem.* 1959; **24**: 1979–1983.
38 Abou Ghalia M, Salem E. Synthesis of *N*-pyridoylamino acid and peptide derivatives with antitubercular activity. Part II. Optically active *N*-nicotinoyl dipeptide derivatives. *Indian J.Chem., Sect. B* 1980; **19B**: 135–138.
39 Bascop S, Laronze J, Sapi J. Synthesis of 2-(3-hydroxypropyl)indol-3-acetic acid and 3-(2-hydroxyethyl)indole-2-propanoic acid by selective functional group transformations. *Synthesis* 2002; **12**: 1689–1694.
40 Addy M, Steinman G, Mallette M. Selectivity in aqueous peptide synthesis by 1-ethyl-3-(3-dimethylaminopropyl) carbodiimide. Model for primordial processes. *Biochim. Biophys. Acta* 1973; **295**: 385–395.
41 Martin WH, Hoover DJ, Armento SJ, Stock IA, McPherson RK, Danley DE, Stevenson RW, Barrett EJ, Treadway JL. Discovery of a human liver glycogen phosphorylase inhibitor that lowers blood glucose in vivo. *Proc. Natl. Acad. Sci. U.S.A.* 1998; **95**: 1776–1781.
42 Lanzetta PA, Alvarez LJ, Reinach PS, Candia OA. An improved assay for nanomole amounts of inorganic phosphate. *Anal. Biochem.* 1979; **100**: 95–97.
43 Hess HH, Derr JE. Assay of inorganic and organic phosphorus in the 0.1–5 nanomole range. *Anal. Biochem.* 1975; **63**: 607–613.

